

# A competitive NISQ and qubit-efficient solver for the LABS problem

Marco Sciorilli,<sup>1</sup> Giancarlo Camilo,<sup>1</sup> Thiago O. Maciel,<sup>1</sup>  
Askery Canabarro,<sup>1</sup> Lucas Borges,<sup>1,2</sup> and Leandro Aolita<sup>1</sup>

<sup>1</sup>*Quantum Research Center, Technology Innovation Institute, Abu Dhabi, UAE*

<sup>2</sup>*Federal University of Rio de Janeiro, Caixa Postal 652, Rio de Janeiro, RJ 21941-972, Brazil*

Pauli Correlation Encoding (PCE) has recently been introduced as a qubit-efficient approach to combinatorial optimization problems within variational quantum algorithms (VQAs). The method offers a polynomial reduction in qubit count and a super-polynomial suppression of barren plateaus. Moreover, it has been shown to feature a competitive performance with classical state-of-the-art methods on MaxCut. Here, we extend the PCE-based framework to solve the Low Autocorrelation Binary Sequences (LABS) problem. This is a notoriously hard problem with a single instance per problem size, considered a major benchmark for classical and quantum solvers. We simulate our PCE variational quantum solver for LABS instances of up to  $N = 44$  binary variables using only  $n = 6$  qubits and a brickwork circuit Ansatz of depth 10, with a total of 30 two-qubit gates, *i.e.* well inside the NISQ regime. We observe a significant scaling advantage in the total time to (the exact) solution of our solver with respect to previous studies using QAOA, and even a modest advantage with respect to the leading classical heuristic, given by Tabu search. Our findings point at PCE-based solvers as a promising quantum-inspired classical heuristic for hard-in-practice problems as well as a tool to reduce the resource requirements for actual quantum algorithms, with both fundamental and applied potential implications.

The Low Autocorrelation Binary Sequences (LABS) problem [1–8] is a well-known NP-hard problem with applications in engineering, communications, and statistical physics. It offers a challenging benchmark for optimization algorithms [2], as finding the optimal global solutions becomes intractable even for moderate problem sizes  $N$ . Classical methods, though powerful for small instances, face significant challenges in finding good solutions for large  $N$ , even when employing massively parallel approaches on CPUs and GPUs [3]. Quantum algorithms have recently been proposed as a potential alternative to classical heuristics for solving combinatorial optimization problems more efficiently [9]. Recent studies indicate that the Quantum Approximate Optimization Algorithm (QAOA) [9] combined with quantum minimum-finding techniques can solve LABS with a runtime scaling of  $\mathcal{O}(1.21^N)$ , outperforming the best-known classical heuristics [4]. However, achieving such an advantage requires a large-scale fault-tolerant quantum computer capable of running a Grover-like amplitude amplification scheme for the quantum minimum-finding subroutine, which is currently not available.

This letter investigates the effectiveness of solving the LABS problem with NISQ devices using Pauli correlation encoding (PCE), a qubit-efficient technique to encode binary variables into quantum states recently introduced in [10]. Notably, PCE encodes  $N$  binary variables using a polynomially smaller number  $n$  of qubits, *i.e.*,  $N = \text{poly}(n)$ , opening up the possibility of exploring large LABS instances with a number of qubits feasible in near-term devices. In particular, using numerical simu-

lations we show that the PCE-based LABS solver has a better exponential scaling in runtime than the QAOA solver and even than the state-of-the-art classical heuristics, given by Tabu search [11].

*The LABS problem.* Given an integer  $N > 2$ , the LABS problem consists in finding a binary sequence  $x \in \{-1, +1\}^{\otimes N}$  of length  $N$  that minimizes the *sidelobe energy*

$$E(x) = \sum_{\ell=1}^{N-1} C_{\ell}^2(x), \quad C_k(x) = \sum_{i=1}^{N-\ell} x_i x_{i+\ell}, \quad (1)$$

where  $C_{\ell}(x)$  is the  $\ell$ -th *autocorrelation* of  $x$ . Notice that  $C_0(x) = N$  for all  $x$ , while  $(N - \ell) \bmod 2 \leq |C_{\ell}(x)| \leq N - \ell$  for  $\ell > 0$ . In statistical physics terms,  $E(x)$  can be interpreted as the energy of a system of  $N$  spins subject to long-range 2- and 4-body interactions known as the Bernasconi model [5]. Equivalently, the problem amounts to maximizing the *merit factor*,

$$F(x) = \frac{N^2}{2E(x)}, \quad (2)$$

which is (half) the ratio between  $C_0(x)^2$  (the *peak*) and the sum of all the other squared autocorrelations (the *sidelobes*). For this reason, sequences with low autocorrelation provide a large peak-to-sidelobe ratio that is a desirable feature for various engineering applications involving pulse modulation [12]. The LABS problem is known to be NP-hard. Solutions are degenerate, and the optimization landscape has a peculiar “golf course” structure [13], plagued by a large number of local minima and extremely isolated global minima [3]. For small enough  $N$ , the

optimal sequence can be found by brute force enumeration of all  $2^N$  possible sequences, but the exponential growth in search space quickly becomes impractical. For odd  $N$ , exact solutions can often (but not always) be found by restricting the search to sequences satisfying the skew-symmetry condition  $x_{(N+1)/2+\ell} = (-1)^\ell x_{(N+1)/2-\ell}$ ,  $\ell \in [1, \frac{(N-1)}{2}]$ , which reduces the effective search space size to  $2^{N/2}$  [1].

In practice, optimal solutions are only known for  $N \leq 66$  [1]. For larger instances, different heuristic algorithms with milder exponential scalings but without optimality guarantees have been employed [14–18]. The best performing one, Memetic Tabu Search [11], has been empirically shown to achieve a runtime scaling of  $\mathcal{O}(1.34^N)$  in the range  $N \leq 40$  [4, 6, 7]. Although these milder scalings suggest attempting larger instances, for  $N > 200$ , the solution quality of classical heuristics has been observed to degrade significantly, and the asymptotic behavior of the maximum merit factor  $F_N := \max_{x \in \{-1, +1\}^{\otimes N}} F(x)$  for large  $N$  remains an open question. Golay conjectured based on the ergodicity postulate the asymptotic upper bound  $F_N \lesssim 12.3248/(8\pi N)^{\frac{3}{2N}}$  as  $N \rightarrow \infty$  [8], but the best known heuristic sequences achieve the much smaller value  $F_N \approx 6.3421$  [19, 20]. Fig. 4 in App. A1 shows a visual summary of the state-of-the-art in LABS solutions using classical solvers.

*Qubit-efficient LABS solver.* Here we propose a qubit-efficient solver for the LABS problem following the *Pauli-correlation encoding* (PCE) framework recently introduced in [10]. We use  $n$  qubits to encode the  $N \leq 3\binom{n}{k}$  binary variables in LABS, where  $k$  is a tunable integer of our choice. This corresponds to a polynomial compression of degree  $k$  with respect to classical encodings, *i.e.*,  $n = \mathcal{O}(N^{1/k})$ . Such a compression is achieved by encoding each binary variable  $x_i$  into the sign of a  $k$ -body correlator of a  $n$  qubit Pauli string  $\Pi_i$  of the form  $X^k \mathbb{1}^{n-k}, Y^k \mathbb{1}^{n-k}, Z^k \mathbb{1}^{n-k}$  (and permutations thereof), namely,

$$x_i := \text{sgn}(\langle \Pi_i \rangle), \quad i \in [N], \quad (3)$$

where  $\text{sgn}$  is the sign function and  $\langle \Pi_i \rangle := \langle \Psi | \Pi_i | \Psi \rangle$  denotes the expectation value of  $\Pi_i$  on a quantum state  $|\Psi\rangle$ . We take  $|\Psi\rangle$  as the output of a parameterized quantum circuit with a brickwork architecture and parameters  $\theta$  to be classically optimized using a variational approach [10] (see App. A2 for details). The goal of the parameter optimization is to minimize the non-linear loss function

$$\mathcal{L} = \sum_{\ell=1}^{N-1} \sum_{i,j=1}^{N-\ell} \tilde{x}_i \tilde{x}_{i+\ell} \tilde{x}_j \tilde{x}_{j+\ell} - \beta \sum_{i=1}^N \tilde{x}_i^2, \quad (4)$$

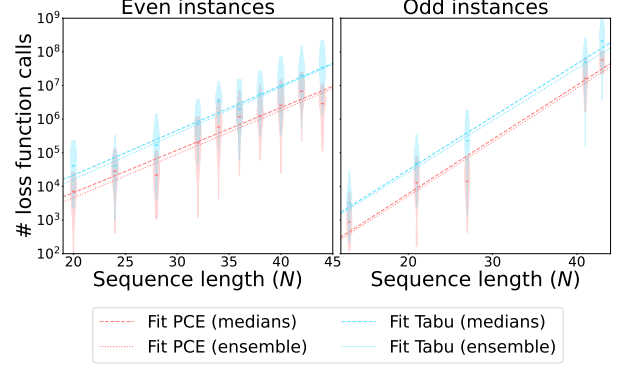


**FIG. 1: Time-to-solution benchmark.** Scaling comparison of the TTS for the quantum LABS solver based on Pauli Correlation Encoding (PCE, red) *vs.* leading classical heuristic based on Tabu Search (Tabu, blue) for even (left) and odd (right) values of  $N$ . Here, TTS is defined as the total number of cost function evaluations required to reach the exact solution [7]. Dashed-dotted lines denote linear regression over the list of median values for each  $N$ , while dotted curves correspond to linear regression over the full dataset of 50 points per instance size. The distribution of points over different initializations is depicted by violin plots at each  $N$ . The fits show a clear exponential scaling in all the cases, with both median and ensemble statistics consistent with a power-law advantage of PCE over the classical baseline. The precise scaling exponents and confidence intervals are shown in Table II in App. A4.

where  $\tilde{x}_i := \tanh(\alpha \langle \Pi_i \rangle)$  is a real-valued relaxation of the binary variable to make it better-suited for gradient-based optimization. The rescaling factor  $\alpha > 1$  is introduced to restore the non-linear behaviour of the  $\tanh$ , given that the  $n$  qubit correlators have magnitude decreasing polynomially with  $n$ . The last term in (4) is a regularization term forcing all correlators away from zero, which was observed to improve the solver’s performance (details on the choice of regularization and the hyperparameters  $\alpha, \beta$  are presented in App. A3). Once the training is complete, the circuit output state is measured and a bit-string  $x$  is obtained via Eq. (3). Then, as a classical post-processing step, we perform one round of single-bit swap search around  $x$  in order to find potential better solutions nearby. The result of the search,  $x^*$ , is the final output of our solver.

*Numerical results.* We have performed numerical simulations of the qubit-efficient quantum solver with  $n = 6$  qubits and second-order polynomial compression ( $k = 2$ ), which allows solving LABS instances of sizes  $N \leq 45$ . The solver encodes the binary variables into correlators of all possible  $n$ -qubit Pauli strings of the form  $X_i X_j, Y_i Y_j$ , and  $Z_i Z_j$  (identities  $\mathbb{1}_\ell$  on the remaining  $n - 2$  qubits are omitted). We tuned the circuit depth to achieve the best pos-

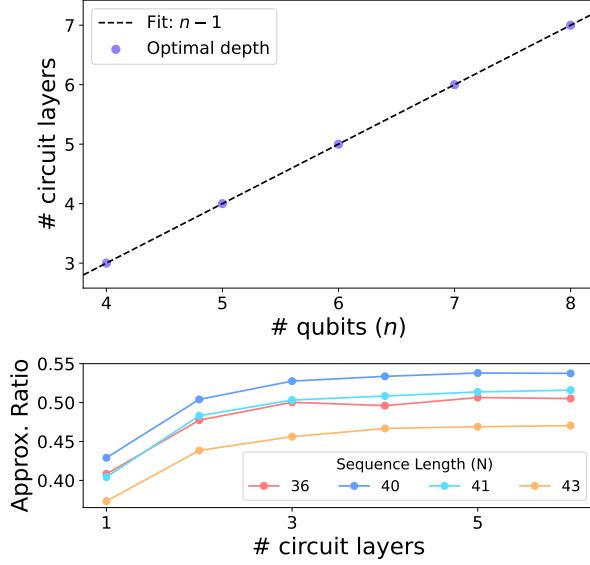


FIG. 2: **Circuit depth scaling.** (Top) Linear scaling of the optimal circuit depth with the number of qubits  $n$  for the qubit-efficient solver with quadratic compression ( $k = 2$ ). This corresponds to a  $\mathcal{O}(\sqrt{N})$  scaling with the problem size  $N$ . (Bottom) For each  $n$  (here illustrated for  $n = 6$ ), the optimal circuit depth was determined by increasing the number of circuit layers until no significant improvement in the average approximation ratio was observed over 1000 runs.

sible approximation ratio as explained in detail in App. A 2. Notably, the optimal circuit depth scales linearly with  $n$  (hence sublinearly with the instance size  $N$ ). This is illustrated in Fig. 2. Based on that, for the demonstrations with  $n = 6$  we fixed the circuit depth to 10 layers (i.e., twice the optimal value in Fig. 2), corresponding to a total of 30 two-qubit gates and 150 parameters.

As our figure of merit, we adopt the time-to-solution (TTS), here defined as the number of cost function evaluations required to observe the exact solution, following the approach outlined in [7]. Similarly, we also study the same quantity but referring to approximate solutions, namely the first and second excited energy levels of Eq. (1), and refer to them as  $\text{TTS}_{1\text{st}}$  and  $\text{TTS}_{2\text{nd}}$ , respectively. To obtain our empirical TTS scaling, we used problem instances with unique canonical solutions (i.e., the ground state is only degenerate due to the inherent symmetries of the problem [7]):  $N \in \{20, 24, 28, 32, 34, 36, 38, 40, 42, 44\}$  for even instances and  $N \in \{13, 21, 27, 41, 43\}$  for odd instances.

When benchmarking different solvers, we used always this same set of instances. We ran the optimization 50 times per instance size  $N$  (except for

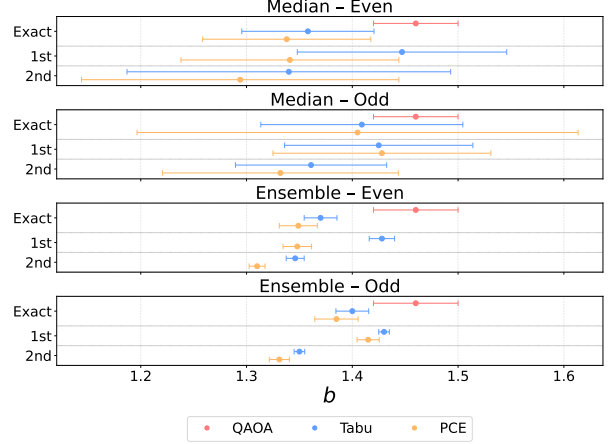


FIG. 3: **TTS scaling for different solvers.** Fitted basis coefficient  $b$  of the exponential scaling in Eq. (5) for our PCE quantum solver, QAOA [4], and Tabu Search (classical) LABS solvers. The corresponding fit data appears in Table II in App. A 4. We report the fits for TTS,  $\text{TTS}_{1\text{st}}$ , and  $\text{TTS}_{2\text{nd}}$  results, corresponding respectively to the exact solution (Exact) and to approximate solutions given by the first (1st) and second (2nd) excited energy levels.

Heuristic	N	b	CI	$R^2$
QAOA [4]	All	1.46	1.42–1.50	>0.94
Tabu [3, 7]	Even	1.358	1.297–1.422	0.97
	Odd	1.409	1.317–1.508	0.97
PCE	Even	<b>1.338</b>	1.261–1.420	0.94
	Odd	<b>1.405</b>	1.212–1.629	0.94

TABLE I: **TTS fit parameters.** Estimated base coefficient  $b$  controlling the exponential scaling of the TTS as in Eq. (5), with respective confidence intervals (CI) and associated  $R^2$  values of the linear fit of  $\log(\text{TTS})$  for the three different solvers (PCE, QAOA, and Tabu Search) for even and odd instances.

$N = 41, 43$ , with 10 runs each), separating the even and odd cases since they are expected to have the same scaling, but with different constant factors [7] (see Fig. 1). We then used this data to fit the exponential curve

$$\text{TTS} = c \cdot b^N \quad (5)$$

by performing linear regression on  $\log(\text{TTS})$  using both the median TTS for each sequence length  $N$ , and also the full data ensemble (and similarly for  $\text{TTS}_{1\text{st}}$  and  $\text{TTS}_{2\text{nd}}$ ). The median fit data for the basis coefficient  $b$  of the exponential scaling for TTS is presented in Table I, while the complete fit data (median and ensemble) for TTS,  $\text{TTS}_{1\text{st}}$  and  $\text{TTS}_{2\text{nd}}$ , are detailed in Tab. II in App. A 4. The results are visually summarized in Fig. 3.

Our results show a clear scaling advantage of PCE compared with the QAOA quantum solver of [4] for both even and odd instances. For a fair comparison, the final quantum amplitude amplification step suggested in [4] was omitted here, since it takes the solver beyond the scope of near-term devices. Here, we used Tabu with a standard implementation without its memetic component, which was observed to not offer any scaling advantage [7], and tenure parameter chosen from the recent GPU implementation in [3]). All the TTS scalings were obtained by local simulations. Remarkably, the PCE results are competitive (within error bars), and in the case of approximate solutions even consistently better, with respect to Tabu search, considered the state-of-the-art classical heuristics for LABS [7]. While minor polynomial advantage factors do not alter the overall exponential scaling, in practice even minor improvements in the basis might play an important role when considering larger problem instances [10] (see details in App. A6). In addition, the approach is promising even as a quantum-inspired algorithm, although in that case one must factor in the significant overhead from classical simulation of the quantum circuit.

In addition, notice that even though the time required to reach optimality is a rigorous metric, it does not fully cover an algorithm's overall performance. For many combinatorial optimization problems, finding a good approximation of the objective function is also hard. Notwithstanding, we analyzed the time-to-solution (TTS) required to reach the second- and third-best objective function values to assess approximate solutions to the LABS problem, referred as  $\text{TTS}_{1\text{st}}$  and  $\text{TTS}_{2\text{nd}}$ , respectively. The advantage over Tabu Search revealed a separation that exceeds the error bars, see App. A4.

Finally, assuming the observed TTS scalings remain the same for larger instances, to run PCE in a quantum hardware, we still need to account the overhead of the gate operations of running quantum circuits multiple times to estimate the loss function and its gradients to a given precision  $\epsilon$ . The gate operations cost are platform-specific, but assuming all gates done sequentially, it scales as  $\mathcal{O}(N)$  (see App. A2); the sample complexity is  $\mathcal{O}(N^7/\epsilon^2)$  (see App. A5); and to estimate the gradient we need  $\mathcal{O}(N)$  calls. Thus, the quantum approach incurs an overall overhead of  $\mathcal{O}(N^9/\epsilon^2)$  to solve the LABS problem.

Even considering the overall overhead of  $\mathcal{O}(N^9)$  when running PCE in a quantum hardware, it is still possible to obtain a preliminary estimate of a crossover point where quantum advantage might be achieved, in App. A6, we showed that, from instance sizes of order of thousands, we would expect advantage in terms of query access to the exact solution, but since the classical solvers can not output exact solutions on instances larger than  $N > 66$ , we might see better (approximate) solutions from the quantum approach sooner.

*Concluding remarks.* Two highlights of our approach are its qubit-efficiency and the strong performance obtained on a hard problem like LABS. With only  $n = 6$  qubits and a total of 30 two-qubit gates, our solver attains a competitive run-time scaling on a hard sequence-length regime. We believe this is what makes the present work relevant: even though PCE-based variational methods have no performance guarantees, the fact that they display such a strong performance not only on MaxCut but now also on a hard benchmark as LABS constitutes a major milestone, urging for further investigations. In this regard, we note that, with the solver variant presented here (which uses a quadratic input-size to qubit-number reduction),  $n = 8$  qubits would be enough to tackle the largest sequence lengths for which LABS has known exact solutions ( $N = 66$ ), while  $n \leq 20$  qubits are enough to challenge even the largest instances solved by state-of-the-art classical heuristics [21]. This regime offers an interesting testbed for our solver as a quantum-inspired heuristic. A challenge there would be the high number of loss-function evaluations required. Possible alternatives to mitigate that could be to incorporate symmetries of the problem in the circuit Ansatz and integrate that with exact geodesic transport for the parameter updates [22]. Other research directions may be problems beyond LABS, such as those in the Quantum Optimization Benchmark Library (QOBLIB) [23]. Our results raise the question of whether PCE has a potential quantum advantage. Although the constant overhead of simulating a full quantum state vector may delay the crossover point after which a runtime advantage becomes evident to larger instance sizes, our method still shows promising performance even in a quantum-inspired setting. All these are exciting questions that our work offers for future work.

---

[1] T. Packebusch and S. Mertens, Low autocorrelation binary sequences, *Journal of Physics A: Mathematical and Theoretical* **49**, 165001 (2016).

[2] I. P. Gent and T. Walsh, CSPLib: A Benchmark Library for Constraints (1999), available online at <http://www.csplib.org/> as prob005.

- [3] Z. Zhang, J. Shen, N. Kumar, and M. Pistoia, New improvements in solving large labs instances using massively parallelizable memetic tabu search (2025), arXiv:2504.00987 [cs.DC].
- [4] R. Shaydulin, C. Li, S. Chakrabarti, M. DeCross, D. Herman, N. Kumar, J. Larson, D. Lykov, P. Minssen, Y. Sun, Y. Alexeev, J. M. Dreiling, J. P. Gaebler, T. M. Gatterman, J. A. Gerber, K. Gilmore, D. Gresh, N. Hewitt, C. V. Horst, S. Hu, J. Johansen, M. Matheny, T. Mengle, M. Mills, S. A. Moses, B. Neyenhuis, P. Siegfried, R. Yalovetzky, and M. Pistoia, Evidence of scaling advantage for the quantum approximate optimization algorithm on a classically intractable problem, *Science Advances* **10**, 10.1126/sciadv.adm6761 (2024).
- [5] Bernasconi, J., Low autocorrelation binary sequences : statistical mechanics and configuration space analysis, *J. Phys. France* **48**, 559 (1987).
- [6] J. E. Gallardo, C. Cotta, and A. J. Fernández, Finding low autocorrelation binary sequences with memetic algorithms, *Applied Soft Computing* **9**, 1252 (2009).
- [7] B. Bošković, F. Brglez, and J. Brest, Low-autocorrelation binary sequences: On improved merit factors and runtime predictions to achieve them, *Applied Soft Computing* **56**, 262 (2017).
- [8] M. Golay, The merit factor of long low autocorrelation binary sequences, *IEEE Transactions on Information Theory* **28**, 543 (1982).
- [9] E. Farhi, J. Goldstone, and S. Gutmann, A quantum approximate optimization algorithm (2014), arXiv:1411.4028 [quant-ph].
- [10] M. Sciorilli, L. Borges, T. L. Patti, D. García-Martín, G. Camilo, A. Anandkumar, and L. Aolita, Towards large-scale quantum optimization solvers with few qubits, *Nature Communications* **16**, 476 (2025).
- [11] F. Glover, Tabu search—part i, *ORSA Journal on Computing* **1**, 190 (1989).
- [12] S. W. Golomb and R. A. Scholtz, Generalized barker sequences, *IEEE Transactions on Information Theory* **11**, 533 (1965).
- [13] S. Mertens and C. Bessenrodt, On the ground states of the bernasconi model, *Journal of Physics A: Mathematical and General* **31**, 3731–3749 (1998).
- [14] Z. Liu, H. Deng, and S. Yang, Search of binary sequences with low aperiodic autocorrelation based on improved multi-objective genetic algorithm, *IET Radar, Sonar & Navigation* (2024).
- [15] Z. Wang and Y. Zhang, Low autocorrelation binary sequences: Best-known peak sidelobe level values, *IEEE Transactions on Aerospace and Electronic Systems* **58**, 3632 (2022).
- [16] B. Jia, F. Ji, W. Jia, and M. Li, Computational search of long skew-symmetric binary sequences with high merit factors, *IEEE Access* **10**, 26269 (2022).
- [17] M. A. Shoaib, S. A. Al-Agtash, and H. M. Al-Khateeb, A hybrid modified sine cosine algorithm using inverse filtering and clipping methods for low autocorrelation binary sequences, in *2022 13th International Conference on Information and Communication Systems (ICICS)* (IEEE, 2022) pp. 324–329.
- [18] J. K.-L. Gancayco, H. R. Tee, J. D. L. Paggabao, and E. P. Dadios, Efficient generation of low autocorrelation binary sequences, in *2020 IEEE Region 10 Conference (TENCON)* (IEEE, 2020) pp. 1018–1023.
- [19] J. Jedwab, D. J. Katz, and K.-U. Schmidt, Advances in the merit factor problem for binary sequences, *Journal of Combinatorial Theory, Series A* **120**, 882 (2013).
- [20] J. Jedwab, D. J. Katz, and K.-U. Schmidt, Littlewood polynomials with small  $l^4$  norm (2013), arXiv:1205.0260 [math.NT].
- [21] B. Pšeničnik, R. Mlinarič, J. Brest, and B. Bošković, Dual-step optimization for binary sequences with high merit factors, *Digital Signal Processing* **165**, 105316 (2025).
- [22] A. Ferreira-Martins, R. M. S. Farias, G. Camilo, T. O. Maciel, A. Tosta, R. Lin, A. Alhajri, T. Haug, and L. Aolita, Variational quantum algorithms with exact geodesic transport, to appear (2025).
- [23] T. Koch, D. E. B. Neira, Y. Chen, G. Cortiana, D. J. Egger, R. Heese, N. N. Hegade, A. G. Cadavid, R. Huang, T. Itoko, T. Kleinert, P. M. Xavier, N. Mohseni, J. A. Montanez-Barrera, K. Nakano, G. Nannicini, C. O’Meara, J. Pauckert, M. Proissl, A. Ramesh, M. Schicker, N. Shimada, M. Takeori, V. Valls, D. V. Bulck, S. Woerner, and C. Zoufal, Quantum optimization benchmark library – the intractable decathlon (2025), arXiv:2504.03832 [quant-ph].
- [24] B. Bošković, F. Brglez, and J. Brest, A GitHub Archive for Solvers and Solutions of the labs problem, For updates, see [https://github.com/borkob/git\\_labs](https://github.com/borkob/git_labs). (2016).
- [25] R. H. Barker, Group synchronization of binary digital system, *Communication theory* , 273 (1953).
- [26] D. Kraft, *A Software Package for Sequential Quadratic Programming*, Deutsche Forschungs- und Versuchsanstalt für Luft- und Raumfahrt Köln: Forschungsbericht (Wiss. Berichtswesen d. DFVLR, 1988).
- [27] D. P. Kingma and J. Ba, Adam: A method for stochastic optimization (2017), arXiv:1412.6980 [cs.LG].
- [28] M. Hollander, D. A. Wolfe, and E. Chicken, *Non-parametric Statistical Methods*, 3rd ed. (John Wiley & Sons, Hoboken, NJ, 2013) includes detailed treatment of the Kolmogorov–Smirnov test.
- [29] J. R. McClean, S. Boixo, V. N. Smelyanskiy, R. Babush, and H. Neven, Barren plateaus in quantum neural network training landscapes, *Nature Communications* **9**, 10.1038/s41467-018-07090-4 (2018).
- [30] F. F. Ferreira, J. F. Fontanari, and P. F. Stadler, Landscape statistics of the low-autocorrelation binarystring problem, *Journal of Physics A: Mathematical and General* **33**, 8635 (2000).

- [31] M. Schuld, V. Bergholm, C. Gogolin, J. Izaac, and N. Killoran, *Evaluating analytic gradients on quantum hardware*, Phys. Rev. A **99**, 032331 (2019).
- [32] M. AbuGhanem, Ibm quantum computers: evolution, performance, and future directions, The Journal of Supercomputing **81**, 687 (2025).
- [33] I. Staff, IonQ Aria: Practical Performance, <https://ionq.com/resources/ionq-aria-practical-performance> (2025), last updated January 8, 2025.
- [34] Intel Corporation, Intel Core i9-14900KS (36M Cache, up to 6.20GHz) – Specifications, <https://www.intel.com/content/www/us/en/products/sku/237504/intel-core-i9-processor-14900ks-36m-cache-up-to-specifications.html> (2024).

## Appendix A: Supplementary Information

### 1. Classical state-of-the-art for LABS

Here we summarize the state-of-the-art of solutions to the LABS problem obtained by classical solvers. We use the data are publicly available at [24], combined with recent improvements in particular instances reported in [3]. For  $N \leq 66$ , solutions with the optimal solution merit factor

$$F_N := \max_{x \in \{-1, +1\}^{\otimes N}} F(x) \quad (\text{A1})$$

can be found using exhaustive search or branch and bound methods. For larger  $N$ , only heuristic solutions are known and there is no proof of optimality. The best known solutions were obtained using the Memetic Tabu Search meta-heuristics [7]. Fig. 4 depicts the best known solutions for  $2 \leq N \leq 449$ . The largest known merit factor is achieved for  $N = 13$  (namely  $F_{13} = 169/12 \approx 14.083$ ) by a so-called *Barker sequence* [25].

### 2. Circuit complexity

Here we provide details on the variational circuit ansatz, the classical optimizer, and strategy to fix the circuit depth for the PCE quantum solver.

*Variational circuit.* For the variational quantum circuit, we employ a hardware-efficient ansatz with the same gate configuration described in [10], namely, RX, RY, and RZ rotations as single-qubit gates and the Mølmer-Sørensen (MS) gate – the native entangling gate of trapped-ion quantum computing platforms, which feature currently the highest fidelities among NISQ devices – for two-qubit interactions.

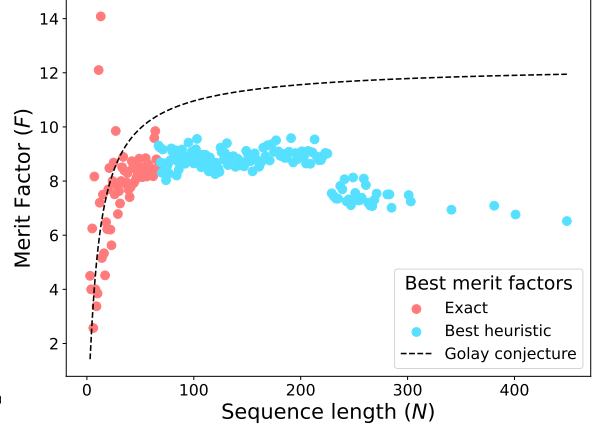


FIG. 4: **LABS state-of-the-art.** Best merit factor vs. problem size  $N$  for classical solvers. Red dots indicate the optimal merit factor  $F_N := \max_{x \in \{-1, +1\}^{\otimes N}} F(x)$  obtained via exact solvers, while blue dots indicate the best known approximation to  $F_N$  obtained via heuristic solvers. The dashed curve is Golay’s conjectured asymptotic upper bound  $\approx 12.3248/(8\pi N)^{\frac{3}{2N}}$  [8].

*Classical optimizer.* For the classical parameter optimization, we used the SLSQP algorithm [26], although analogous performance was observed using the Adam optimizer [27].

*Circuit depth scaling.* To determine a suitable circuit depth, we chose per each circuit size 4 different “hard” instances  $N$  (namely, 2 even and 2 odd) as mentioned in the main text and solved them using the PCE quantum solver with a circuit ansatz having an increasing number of layers. In each instance and number of layers, we run the solver with 1000 different random initializations and, for each run, record the corresponding fraction of the optimal merit factor  $F_N$  achieved (i.e., *approximation ratio*). Then we used the Kolmogorov–Smirnov test [28] to identify the point after which there were no more statistically significant improvements in the distributions of the approximation ratios, which we refer to as optimal circuit depth. As shown in Fig. 2, the optimal depth was observed to scale linearly with the number of qubits  $n$ , and therefore sublinearly with the instance size  $N$ . Interestingly, a linear scaling of the depth in  $n$  is also known to lead to approximate Haar randomness [29].

### 3. Regularization term and hyperparameters

In this section, we discuss the form of the regularization term and the tuning of hyperparameters  $\alpha$  and  $\beta$  appearing in the loss function (4).



*Regularization term.* We first notice from Eq. (1) that the energy spectrum of LABS is strictly positive. In our formulation of the problem, however, the binary variables are relaxed to (hyperbolic tangents of) expectation values of Pauli operators, which take real values in the interval  $[-1, 1]$ . Therefore, if one tries to minimize the loss function 4 naively without any penalization term ( $\beta = 0$ ), we quickly converge to the trivial solution  $\tilde{x}_i = 0$  for all  $i$  (where all the expectation values go to 0), which does not offer any valuable insight for the binary version of the problem. For this reason, we introduced a regularization term with a positive coefficient  $\beta$  penalizing this strong attractor. For simplicity, we used the simple  $\ell_2$ -norm penalization  $\beta \sum_{i=1}^N \tilde{x}_i^2$ .

*Tuning of  $\alpha$  and  $\beta$ .* For each instance and hyperparameter size, we ran the solver using 1000 distinct random initializations. For every run, we recorded the achieved fraction of the optimal merit factor  $F_N$ , referred to as the *approximation ratio*, as reported in Fig. 5. Next, we used the Kolmogorov–Smirnov test [28] to identify the hyperparameter size beyond which further increases did not result in statistically significant improvements in the approximation ratio distributions. As shown in Fig. 5 for the case of  $n = 6$  qubits, this resulted in values  $\alpha = 1.5n$  and  $\beta = 12$ . For the purpose of our estimation of the Time-To-Solution (TTS), these were the values used through our numerical benchmarks.

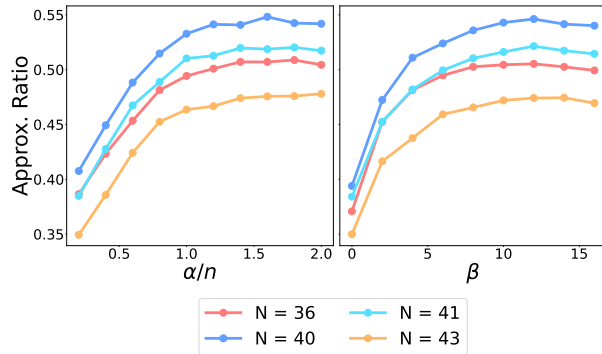


FIG. 5: **Hyperparameters tuning.** (Left) Tuning of the rescaling parameter  $\alpha$ ; (Right) Tuning of the penalization constant  $\beta$ . In each case, we fixed the number of qubits to  $n = 6$ , the circuit depth to 10, and the optimal value was determined by increasing the corresponding parameter until no significant improvement in the average approximation ratio was observed over 1000 runs.

#### 4. PCE as a LABS approximate solver

For many combinatorial optimization problems, finding a good approximation of the objective func-

tion is also hard. Unlike the MaxCut problem, a rigorous proof of the approximation hardness for the LABS problem is still lacking. However, numerical studies and its unique optimization landscape strongly suggest that LABS is likely difficult to approximate (see [30]).

Even though the time required to reach optimality is a rigorous metric, it does not fully cover an algorithm’s overall performance. Notwithstanding, we evaluate our solver’s performance in approximating solutions to the LABS problem by analyzing the time-to-solution (TTS) required to reach the second- and third-best objective function values (*i.e.*, the first- and second-excited energy levels of Eq. 1) to assess approximate solutions to the LABS problem, here referred as TTS<sub>1st</sub> and TTS<sub>2nd</sub>, respectively.

In both estimates, we observed an exponential behavior similar to the exact solution. However, the advantage over Tabu Search revealed a separation that exceeds the error bars, see Fig. 6, with the corresponding exponential bases reported in Tab. II. We were unable to obtain the corresponding data for QAOA due to the highly demanding nature of its classical simulations at this scale [4].

#### 5. Shot complexity

Given  $\varepsilon, \delta > 0$ , and a vector  $\theta$  of variational parameters, consider the problem of estimating  $\mathcal{L}$  up to additive precision  $\varepsilon$  and with statistical confidence  $1 - \delta$ . For each Pauli correlator  $\langle \Pi_i \rangle$ ,  $i \in [N]$ , assume that, with confidence  $1 - \delta$ , one has an unbiased estimator  $\Pi_i^*$  with statistical error at most  $\eta > 0$ , *i.e.*,

$$|\Delta \langle \Pi_i \rangle| := |\langle \Pi_i \rangle - \Pi_i^*| \leq \eta. \quad (\text{A2})$$

The corresponding error in the loss function is  $\Delta \mathcal{L} := \mathcal{L} - \mathcal{L}^*$ , with  $\mathcal{L}^*$  given by (4) calculated using  $\Pi_i^*$  instead of  $\langle \Pi_i \rangle$ . The multivariate Taylor theorem ensures that there is a  $\xi \in [-1, 1]^N$  such that

$$\Delta \mathcal{L} = \sum_{i \in [N]} \left. \frac{\partial \mathcal{L}}{\partial u_i} \right|_{u_i = \xi} \Delta \langle \Pi_i \rangle. \quad (\text{A3})$$

For the loss function (4), using  $\tanh(x) \leq 1$  and  $\frac{d}{dx} \tanh(x) = \text{sech}^2(x) \leq 1$ , one can show that  $\left| \frac{\partial \mathcal{L}}{\partial u_i} \right|_{\xi_i} \leq 2\alpha [N(N-1) + \beta]$ . As a result,

$$|\Delta \mathcal{L}| \leq 2\eta \alpha N [N(N-1) + \beta] \quad (\text{A4})$$

follows immediately from the triangle inequality together with (A2). To ensure  $|\Delta \mathcal{L}| \leq \varepsilon$  we then require that

$$\eta \leq \frac{\varepsilon}{2\alpha [N(N-1) + \beta]}. \quad (\text{A5})$$

Solution	Heuristic	Type	N	b	CI	c	CI	$R^2$
Exact	QAOA [4]	All	All	1.46	1.42–1.50	–	–	>0.94
	Tabu	Median	Even	1.358	1.297–1.422	47.6	9.7–232.4	0.97
			Odd	1.409	1.317–1.508	21.9	3.6–133.6	0.97
		Ensemble	Even	1.370	1.355–1.386	29.5	19.8–44.2	0.78
			Odd	1.400	1.384–1.415	21.4	15.8–28.9	0.88
	PCE	Median	Even	<b>1.338</b>	1.261–1.420	19.2	2.5–150.4	0.94
			Odd	<b>1.405</b>	1.082–1.826	3.6	0.04–319.3	0.94
		Ensemble	Even	<b>1.348</b>	1.335–1.362	11.7	7.5–18.4	0.69
			Odd	<b>1.385</b>	1.365–1.406	3.2	2.2–4.8	0.84
1st	Tabu	Median	Even	1.447	1.351–1.549	3.7	0.3–39.5	0.95
			Odd	<b>1.425</b>	1.339–1.517	4.8	0.7–33.9	0.99
		Ensemble	Even	1.428	1.416–1.440	4.4	3.3–5.9	0.77
			Odd	1.430	1.425–1.435	1.4	3.6–4.4	0.91
	PCE	Median	Even	<b>1.341</b>	1.242–1.448	12.2	0.9–173.6	0.91
			Odd	1.428	1.242–1.448	2.2	0.9–173.6	0.98
		Ensemble	Even	<b>1.348</b>	1.335–1.362	7.9	5.5–11.2	0.69
			Odd	<b>1.415</b>	1.405–1.426	2.2	1.7–2.7	0.89
2nd	Tabu	Median	Even	1.340	1.196–1.502	24.3	0.5–1260.2	0.81
			Odd	1.361	1.291–1.434	12.0	2.3–61.7	0.99
		Ensemble	Even	1.346	1.338–1.355	16.0	12.8–20.0	0.65
			Odd	1.350	1.345–1.355	15.0	13.5–16.7	0.91
	PCE	Median	Even	<b>1.294</b>	1.152–1.452	18.7	0.3–1024.6	0.77
			Odd	<b>1.332</b>	1.225–1.448	11.9	0.9–161.7	0.98
		Ensemble	Even	<b>1.349</b>	1.331–1.367	9.8	8.0–12.1	0.73
			Odd	<b>1.331</b>	1.321–1.340	10.2	8.1–12.7	0.85

TABLE II: **TTS for the exact solution, first-, and second-excited energy.** Estimated base value  $b$  and constant  $c$  controlling the exponential scaling in Eq. (5), and associated  $R^2$  values for the TTS linear fit across three different algorithms (PCE, and Tabu Search) for even and odd instances.

The minimum number  $S$  of samples needed to achieve such precision can be upper-bounded by standard arguments using the union bound and Hoeffding’s inequality, which gives  $S \leq (2/\eta^2) \log(2N/\delta)$ . Then, by virtue of Eq. (A5), it suffices to take

$$S \geq \frac{8\alpha^2 N^2}{\varepsilon^2} [N(N-1) + \beta]^2 \log\left(\frac{2N}{\delta}\right). \quad (\text{A6})$$

This is the general form of our upper bound and guarantees  $P(|\Delta\mathcal{L}| \leq \varepsilon) \geq 1 - \delta$ . Recall from App. A 3 that  $\alpha = 1.5n = \mathcal{O}(\sqrt{N})$ . We also reiterate that this a loose upper bound and, in practice, the actual number of samples is expected to have a better scaling in  $N$ .

## 6. Quantum-classical crossover point

In our numerical results, we observed a competitive TTS scaling compared to Tabu Search in terms of query access to the loss function. However, each quantum query incurs an overhead given by gate operations and the sample complexity to guarantee that all expectation values are estimated within desired precision. Furthermore, our approach also need an estimation of the gradient, usually done in the context of VQA using parameter-shift-rule [31]. Assuming the observed TTS scalings remain the same for larger instances, we can use the circuit and sample complexity estimates in Apps. A 2 and A 5 to determine the crossover point in which we expect to observe a quantum advantage in query complexity. Our estimation in Tab. III considers the scaling obtained for the the median of the even instances, as it has a better value of the  $R^2$ , and the crossing



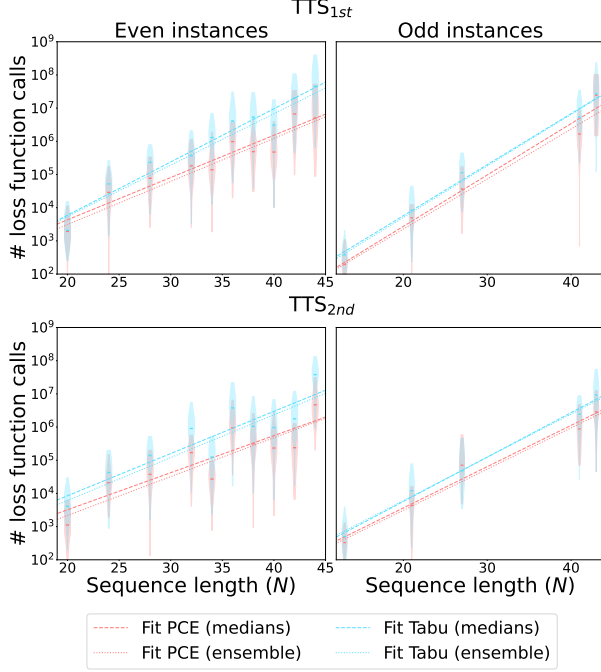


FIG. 6: **Time-to-solution benchmark.** Scaling comparison of the  $TTS_{1st}$  and  $TTS_{2nd}$  for the quantum LABS solver based on Pauli Correlation Encoding (PCE, red) *vs.* Tabu Search (Tabu, blue) for even (left) and odd (right) values of  $N$ . Here, TTS is defined as the total number of cost function evaluations required to reach the exact solution [7]. Dashed-dotted lines denote linear regression over the list of median values for each  $N$ , while dotted curves correspond to linear regression over the full dataset of 50 points per instance size. The distribution of points over different initializations is depicted by violin plots at each  $N$ . The fits show a clear exponential scaling in all the cases, with both median and ensemble statistics consistent with a power-law advantage of PCE over the classical baseline. The precise scaling exponents and confidence intervals are shown in Tab. II.

points for advantage are given in terms of query complexity and walltime for two different quantum hardware platforms: superconducting (SC) and trapped-ion (TI) qubits. For superconducting qubits, we take each layer to be executed in parallel, while, for trapped-ions, each gate is considered as executed sequentially. For the estimation of the walltime, we assumed an overhead of  $5 \times 10^2$  for superconduct-

ing qubits [32], and  $6 \times 10^6$  for trapped ion [33], when comparing to a cycle of a current day CPU [34]. In addition, we disregarded any extra overhead due to error mitigation that the quantum approach may need. This was done both because a detailed estimation would be heavily platform dependent, and because the actual impact that error noise have in the training of our specific VQA (and so the level of error mitigation actually needed) is still an open question. While the size instance reported in Tab. III give us the expected crossing point of the scaling of the two methods, the observed improvement in performance of PCE for obtaining solutions beyond the exact one also gives us hope of achieving better approximation ratios than the classical algorithm already at considerably smaller problem sizes, especially in light of the dramatic degradation of performance of Tabu Search at instances on the size of few hundreds. Finally, as observed in [10], while our estimation of the shot complexity gives us an upper bound. We expect this bound to be quite loose, and to need to run the quantum circuits fewer times, lowering therefore the crossing point.

Solution	QPU	Adv. Type	$N_*$
Exact	SC	Walltime	6022
		Queries	5575
	TI	Walltime	7024
		Queries	5951
1st	SC	Walltime	1004
		Queries	915
	TI	Walltime	1191
		Queries	977
2nd	SC	Walltime	2314
		Queries	2125
	TI	Walltime	2724
		Queries	2268

TABLE III: **Crossover points.** Estimated instance size  $N_*$  after which the PCE solver is expected to outperform the classical Tabu search solver in terms of total walltime or total number of queries to the loss function for two different quantum hardware platforms: superconducting qubits (SC) and trapped ion (TI) qubits.